Elucidating syntrophic butyrate-degrading populations in anaerobic digesters using stable isotope-informed genome-resolved metagenomics

Ryan M. Ziels[1,2,#], Masaru K. Nobu[3], Diana Z. Sousa[4]

[1] Department of Civil Engineering, University of British Columbia, Vancouver, Canada

[2] Department of Civil and Environmental Engineering, University Washington, Seattle, USA

[3] Bioproduction Research Institute, National Institute of Advanced Industrial Science and Technology, Tsukuba, Japan

[4] Laboratory of Microbiology, Wageningen University & Research, Wageningen, Netherlands

#Corresponding Author:

Email: ziels@mail.ubc.ca

Running Title: DNA-SIP Metagenomics of Anaerobic Butyrate-Degraders

Abstract:

Linking the genomic content of uncultivated microbes to their metabolic functions remains a critical challenge in microbial ecology. Resolving this challenge has implications for improving our management of key microbial interactions in biotechnologies such as anaerobic digestion, which relies on slow-growing syntrophic and methanogenic communities to produce renewable methane from organic waste. In this study, we combined DNA stable isotope probing (SIP) with genome-centric metagenomics to recover the genomes of populations enriched in ^{13}C after feeding ^{13}C-labeled butyrate. Differential abundance analysis on recovered genomic bins across the SIP metagenomes identified two metagenome-assembled genomes (MAGs) that were significantly enriched in the heavy ^{13}C DNA. Phylogenomic analysis assigned one MAG to the genus *Syntrophomonas*, and the other MAG to the genus *Methanothrix*. Metabolic reconstruction of the annotated genomes showed that the *Syntrophomonas* genome encoded all the enzymes for beta-oxidizing butyrate, as well as several mechanisms for interspecies electron transfer via electron transfer flavoproteins, hydrogenases, and formate dehydrogenases. The *Syntrophomonas* genome shared low average nucleotide identity (< 95%) with any cultured representative species, indicating it is a novel species that plays a significant role in syntrophic butyrate degradation within anaerobic digesters. The *Methanothrix* genome contained the complete pathway for aceticlastic methanogenesis, indicating that it was enriched in ^{13}C from syntrophic acetate transfer. This study demonstrates the potential of stable-isotope-informed genome-resolved metagenomics to elucidate the nature of metabolic cooperation in slow-growing uncultured microbial populations, such as syntrophic bacteria and methanogens, that are important to waste treatment as well as global carbon cycling.

41 **Importance:**

42 Predicting the metabolic potential and ecophysiology of mixed microbial communities remains a
43 major challenge, especially for slow-growing anaerobes that are difficult to isolate. Unraveling the
44 *in-situ* metabolic activities of uncultured species could enable a more descriptive framework to
45 model substrate transformations by microbiomes, which has broad implications for advancing the
46 fields of biotechnology, global biogeochemistry, and human health. Here, we investigated the *in-*
47 *situ* function of mixed microbiomes by combining DNA-stable isotope probing with
48 metagenomics to identify the genomes of active syntrophic populations converting butyrate, a C_4
49 fatty acid, into methane within anaerobic digesters. This approach thus moves beyond the mere
50 presence of metabolic genes to resolve '*who is doing what*' by obtaining confirmatory assimilation
51 of labeled substrate into the DNA signature. Our findings provide a framework to further link the
52 genomic identities of uncultured microbes with their ecological function within microbiomes
53 driving many important biotechnological and global processes.
54
55
56
57
58
59

Introduction:

Linking microbial genomic identity with ecological function is considered a 'Holy Grail' in microbial ecology (1), and has broad implications for improving our ability to manage microbial communities in engineered biotechnologies. Anaerobic digestion is an example of a biotechnology that enables resource recovery from organic waste by generating methane gas as a renewable biofuel, and thus plays a role in establishing a circular economy (2). The production of methane in anaerobic digestion is executed through a series of trophic interactions constituting a metabolic network of fermenting bacteria, syntrophic acetogens, and methanogenic archaea (3, 4). Metabolic reconstructions based on shotgun metagenomic sequencing data have highlighted potential partitioning of functional guilds within anaerobic digester microbiomes (4). Yet, our understanding of the ecophysiology of the microorganisms present in anaerobic digesters is limited by the high community complexity and lack of cultured representatives (4). Elucidating the nature of interspecies interactions between different trophic groups in the anaerobic digester metabolic network could help to better understand and optimize the conversion of organic wastes into renewable methane.

The terminal steps in the anaerobic metabolic network — syntrophy and methanogenesis — are considered rate limiting steps for the production of methane from organic substrates (5). The syntrophic oxidation of fatty acids is also responsible for a considerable portion of carbon flux in methanogenic bioreactors, as fatty acids are often produced during fermentation of mixed organic substrates (6). The accumulation of fatty acids in anaerobic digesters is often responsible for a reduction in pH and process instability (3). In particular, syntrophic degradation of the 4-carbon fatty acid, butyrate, can be a bottleneck for anaerobic carbon conversion, as this metabolism occurs

83 at the thermodynamic extreme. Butyrate degradation to acetate and hydrogen is
84 thermodynamically unfavorable under standard conditions ($\Delta G^{\circ\prime} = 53$ kJ/mol), and only yields -
85 21 kJ/mol under environmental conditions typical of anaerobic bioreactors (pH 7, 1 mM butyrate
86 and acetate, 1 Pa H_2). Thus, cooperation with acetate- and hydrogen-scavenging methanogenic
87 partners is necessary to maintain thermodynamic favorability. Cultured representative species
88 carrying out syntrophic fatty acid oxidation are potentially underrepresented due to their slow cell
89 yields and difficulty of isolation in the lab (7). Insofar, only two mesophilic (*Syntrophomonas* and
90 *Syntrophus*) and two thermophilic (*Syntrophothermus* and *Thermosyntropha*) genera (12 bacterial
91 species total) have been shown to oxidize butyrate in syntrophic cooperation with methanogenic
92 archaea, and they all belong to the families *Syntrophomonadaceae* and *Syntrophaceae* (7). Despite
93 their major roles in processing carbon within anaerobic bioreactors, many syntrophic fatty acid-
94 oxidizing bacteria have evaded detection with quantitative hybridization-based techniques (8),
95 which is likely due to their low biomass yields (9) or our incomplete knowledge of active
96 syntrophic populations within anaerobic digesters (10). Broad metagenomic surveys of anaerobic
97 digester communities have similarly observed poor resolution of syntrophic populations, owing to
98 their low abundance (4, 11). Thus, highly sensitive culture-independent approaches are needed to
99 expand our understanding of the ecophysiology of syntrophic populations to better control and
100 predict metabolic fluxes in anaerobic environments.
101
102 Recently, we demonstrated the potential of combining DNA-stable isotope probing (SIP) with
103 genome-resolved metagenomics to identify syntrophic populations degrading the long-chain fatty
104 acid, oleate ($C_{18:1}$), within anaerobic digesters (12). Stable-isotope informed metagenomic
105 sequencing can enrich metagenomic libraries with genomic sequences of actively-growing

106 microbes that incorporate ^{13}C into their biomass from an added labeled substrate (13), and thus
107 allows for a 'zoomed in' genomic view of low-abundance populations such as syntrophs. We also
108 demonstrated that this approach was amenable for recovering high-quality microbial genomes
109 using a differential-coverage based binning approach, as genomes from active microbes have low
110 abundance in DNA from ^{12}C controls but are enriched in ^{13}C-ammended treatments (12). Here, we
111 applied stable-isotope informed metagenomics to resolve the genomic makeup of active syntrophic
112 butyrate-degrading populations within an anaerobic digester. We utilized biomass collected from
113 the same anaerobic digesters as were previously used for DNA-SIP with oleate (12) at a similar
114 time point, thus allowing for genomic comparisons using a multi-substrate SIP dataset. This
115 approach identified potential metabolic flexibility in syntrophic populations processing multiple
116 fatty acids within the anaerobic digesters, and elucidated the genomic identity of syntrophic
117 partnerships between active methanogens and bacteria.
118
119
120
121
122
123
124
125
126

Results and Discussion:

DNA stable isotope probing (SIP) of methanogenic microcosms with ^{13}C-labeled butyrate

Anaerobic digester contents from a pulse-fed and continuous-fed anaerobic digester were incubated in duplicate microcosms that were spiked with either ^{12}C or ^{13}C-labelled butyrate (40 mM) for approximately 50 hours. The added butyrate was converted into methane at >80% conversion efficiency based on COD recovery (Supplemental Figure S1). After the 50 hr incubation, the contents of the microcosms were sacrificed for DNA extraction, density-gradient centrifugation, and fractionation.

The abundance of 16S rRNA genes of the known butyrate-degrading genus, *Syntrophomonas*, was quantified across density gradient fractions using qPCR to identify DNA fractions that were enriched in ^{13}C (Supplemental Figure S2). Density fractions with a buoyant density from 1.70 to 1.705 had 2.0 to 2.2-times higher *Syntrophomonas* 16S rRNA genes (normalized to maximum concentration) than the ^{12}C controls. Those DNA fractions were selected from each SIP microcosm for metagenomic sequencing, as well as for 16S rRNA gene amplicon sequencing.

The microbial communities in the heavy density-gradient fractions were assessed through paired-end 16S rRNA gene amplicon sequencing for all ^{12}C- and ^{13}C-incubated duplicate microcosms (Figure 1). Differential abundance analysis of OTU read counts with DESeq2 (14) showed that approximately 50% (7 of 15) of the significantly-enriched (p<0.05) OTUs in the ^{13}C heavy DNA samples relative to ^{12}C were taxonomically classified as *Syntrophomonas* for the pulse-fed digester (Supplemental Figure S3). For the continuous-fed digester, approximately 40% of the ^{13}C-enriched OTUs (7 of 17) were assigned to *Syntrophomonas* (Supplemental Figure S4).

Additionally, two ^{13}C-enriched OTUs in both digesters were assigned to *Methanothrix* (formerly *Methanosaeta*), which likely scavenge the ^{13}C-acetate generated by *Syntrophomonas* during ^{13}C-butyrate degradation. While one previous study observed that *Syntrophaceae* was predominantly enriched in anaerobic digester granular sludge incubated with ^{13}C-labeled butyrate (10), various other studies also detected *Syntrophomonadaceae* populations as active syntrophic butyrate degraders in anaerobic digester sludge using ^{14}C-labeled butyrate and MAR-FISH (15), in anaerobic digester sludge through SIP using ^{13}C-labeled oleate (12), and in rice paddy soil with SIP using ^{13}C-labeled butyrate (16). In the latter two studies, acetate-scavenging partners (*Methanothrix* and *Methanosarcinaceae*) were also enriched. Indeed, syntrophic interaction with acetoclastic methanogens is beneficial as acetate accumulation can thermodynamically hinder butyrate oxidation (*e.g.*, ΔG exceeds the theoretical threshold for catabolism [-10 kJ/mol] when acetate accumulates beyond 10 mM [pH 7, 1mM butyrate, and 1Pa H_2]). Notably, H_2- and formate-consuming methanogens necessary for syntrophy are not detected during degradation of ^{13}C butyrate because these archaea utilize CO_2 as a carbon source.

Our results also found ^{13}C-enriched OTUs from lineages not known to degrade butyrate under methanogenic conditions: *Treponema, Luteimonas, Thauera, Christensenellaceae* (*Firmicutes*), and *Anaerolineaceae* (*Chloroflexi*) (Supplemental Figures 3 and 4). Other studies using ^{13}C-butyrate also detected enrichment of populations likely unable to degrade butyrate, including *Tepidanaerobacter* and *Clostridium* in a thermophilic anaerobic digester operated at 55ºC (10) and *Chloroflexi* and *Planctomycetes* in rice paddy soil (16). Members of *Tepidanaerobacter* and *Clostridium* are known to syntrophically oxidize acetate under thermophilic conditions (17), and may have thus been enriched in ^{13}C RNA from ^{13}C-labeled acetate produced during the beta-

173 oxidation of labeled butyrate in the study by Hatamoto *et al.* (10). Similarly, the *Chloroflexi* and
174 *Planctomycetes* populations were hypothesized to have become enriched due to cross-feeding of
175 intermediate metabolites like acetate in the rice paddy soil (16). Thus, the 'peripheral' populations
176 detected in our study may grow on cell-decay products, as genome-resolved metagenomics
177 recently indicated that some uncultured *Anaerolineaceae* species are likely fermenters in anaerobic
178 digesters (18). These results thus suggest that carbon cross-feeding may occur between multiple
179 microbial groups during the syntrophic degradation of butyrate in anaerobic digesters.
180
181 *Identifying active metagenome-assembled genomes (MAGs) in SIP metagenomes*
182 Metagenomic sequencing of heavy DNA from duplicate ^{13}C and ^{12}C-butyrate amended
183 microcosms yielded an average of 30 M paired reads per sample for both digesters (n=8)
184 (Supplemental Table S1). The filtered reads from heavy ^{13}C DNA were co-assembled, yielding a
185 total assembly length of 516 Mb of contigs larger than 1 kb, with an average (N50) contig length
186 of 5 kb. The fraction of filtered short reads that mapped to the co-assembly were 66% ± 3 (s.d) and
187 69% ± 1 for the ^{12}C and ^{13}C metagenomes, respectively (n=4 each) (Supplemental Table S1). The
188 co-assembly generated from ^{13}C reads thus captured much of the genomic information present in
189 the heavy DNA fractions.
190
191 The assembled metagenomic contigs were organized into 160 genomic bins at various levels of
192 completion and redundancy (Supplemental File 1). Differential abundance analysis of the mapped
193 read counts for the bins across the ^{13}C and ^{12}C metagenomes with DESeq2 (14) identified two
194 genomic bins that were significantly ($p < 0.05$) enriched in ^{13}C DNA (Table 1). Based on suggested
195 completion and redundancy metrics for metagenome-assembled-genomes (MAGs) (19), one

196 genomic bin is classified as a high-quality MAG (completion >90%, redundancy <10%), while the
197 other is a medium-quality MAG (completion >50%, redundancy <10%). Taxonomic classification
198 with CheckM (20) assigned one of the MAGs to the genus *Syntrophomonas*, and the other to
199 *Methanothrix* (Table 1).
200
201 Phylogenomic placement of the ^{13}C-enriched *Syntrophomonas* BUT1 MAG was consistent with
202 its taxonomic assignment, as it was located in the *Syntrophomonas* genome cluster within the
203 family *Syntrophomonadaceae* (Figure 2). The closest relative to *Syntrophomonas* BUT1 based on
204 single-copy marker genes was *Syntrophomonas* PF07, which was a genomic bin enriched in ^{13}C
205 from DNA-SIP with labelled oleate ($^{13}C_{18:1}$) with sludge from the same pulse-fed digester used in
206 this study (12). A high average nucleotide identity (ANI) of 99% was observed between the
207 *Syntrophomonas* BUT1 and *Syntrophomonas* PF07 genomes (Supplemental Figure S5),
208 suggesting that these two organisms likely originated from the same sequence-discrete population
209 (21). The next closest relative of *Syntrophomonas* BUT1 based on the phylogenomic analysis was
210 *Syntrophomonas zehnderi* OL-4 (Figure 2), which was isolated from an oleate-fed anaerobic
211 granular sludge bioreactor (22). However, the ANI between *Syntrophomonas* BUT1 and
212 *Syntrophomonas zehnderi* OL-4 was below 95% (Supplemental Figure S5), suggesting that these
213 two organisms were different species (23). Thus, the active butyrate-degrading bacterial MAG
214 identified in this study is distinct from any species obtained in isolation at this time. The detection
215 of the sequence-discrete population of *Syntrophomonas* BUT1 within heavy ^{13}C-DNA from
216 experiments with both labelled butyrate and oleate indicate that this syntrophic population could
217 be metabolically flexible; that is, it may grow on fatty-acids of variable length and degree of
218 saturation. This finding has implications for current frameworks for mathematical modeling of

anaerobic digesters, which typically assume that LCFA and butyrate-degrading populations are distinct (24). Thus, the incorporation of genomic and functional characterization, as obtained through DNA-SIP genome-resolved metagenomics, may help to improve our ability to accurately model anaerobic digestion processes by accounting for metabolic flexibility within key functional guilds.

A phylogenomic analysis of the ^{13}C-enriched *Methanothrix* BUT2 based on archaeal single-copy marker genes placed the MAG within the genus *Methanothrix,* consistent with its taxonomic assignment (Figure 3). *Methanothrix* BUT2 was closely clustered with the genome of *Methanothrix soehngenii* GP6, along with four MAGs reported in the study of Parks *et al.* (25). Congruent with the phylogenomic analysis, *Methanothrix* BUT2 shared an ANI over 98% with *Methanothrix soehngenii* GP6 and the same with four MAGs from Parks *et al.* (25) (*M.* UBA243, *M.* UBA458, *M.* UBA70, *M.* UBA356), indicating that these genomes likely form a sequence-discrete population (Supplemental Figure S5). A second, closely-related population including three MAGs from Parks *et al.* (25) (*M.* UBA372, *M.* UBA332, *M.* UBA553) shared an ANI of 96% with the *Methanothrix* BUT2 population (Supplemental Figure S5).

DNA-SIP using ^{13}C-labeled oleate with the same anaerobic digester biomass as this study did not identify any ^{13}C-enriched methanogenic archaea in the genome-resolved metagenomic analysis (12). One possible explanation for the higher relative enrichment of methanogens on ^{13}C-butyrate versus ^{13}C-oleate could be the higher fraction of overall free-energy partitioned towards methanogens during anaerobic butyrate degradation versus oleate degradation. For the overall conversion of 1 mole of butyrate to CO_2 and CH_4 at environmental conditions in anaerobic

242 digesters, the thermodynamic yields would be -21.1, -9.4, and -58.9 kJ for the acetogenic bacteria,
243 hydrogenotrophic methanogens, and aceticlastic methanogens, respectively (Table 2). For similar
244 conversion of 1 mole of oleate, the thermodynamic yields would be -219.9, -70.6, and -264.9 kJ
245 respectively (Table 2). Thus, the acetogen would gain a much lower percentage of the overall free
246 energy yield from conversion of butyrate (24%) than oleate (40%). As cell yield can depend on
247 free-energy (26), the lower yield of the butyrate degradation would likely leave a higher fraction
248 of acetate for assimilation by aceticlastic methanogen compared to oleate. Supporting this, the
249 relative energy yield of aceticlastic methanogens compared to the acetogen is higher for conversion
250 of butyrate (0.45) than oleate (0.32). As the stable-isotope informed analysis utilized in this study
251 depended on heterotrophic incorporation of the added ^{13}C into biomass, it was not expected that
252 autotrophic (i.e. hydrogenotrophic) methanogens would be enriched in the heavy ^{13}C DNA
253 because no CO_2 is produced during butyrate beta-oxidation (Table 2). Comparing the enriched
254 communities from DNA SIP with different fatty acids, along with bicarbonate, could potentially
255 highlight differences in energy partitioning between syntrophic bacteria and different archaeal
256 partners.
257
258 *Metabolic potential of ^{13}C-enriched MAGs*
259 Functional annotation and metabolic reconstruction of the ^{13}C-enriched MAGs revealed their
260 capacity to metabolize the labeled butyrate into methane through syntrophic cooperation (Figure
261 4).
262
263 A complete pathway for butyrate β-oxidation was annotated in *Syntrophomonas* BUT1, indicating
264 that this MAG was capable of metabolizing the added ^{13}C-butyrate (Figure 4). Notably, several

265 homologues were detected for genes in the β-oxidation pathway (Supplemental File 2). *S.* BUT1
266 genome encodes 6 acyl-CoA-transferases, 7 acyl-CoA dehydrogenases, 8 enoyl-CoA hydratases,
267 5 3-hydroxybutyryl-CoA dehydrogenases, and 10 acetyl-CoA acetyltransferases (Supplemental
268 File 2). The presence of homologous β-oxidizing genes was also observed in the type-strain *S.*
269 *wolfei* ssp. *wolfei* Göttingen DSM 2245B (27). The large number of homologous β-oxidizing genes
270 may afford *S.* BUT1 flexibility to metabolize multiple fatty acid substrates, as its genomic
271 population was detected in heavy ^{13}C DNA during SIP with both butyrate (C_4) and oleate (C_{18})
272 (12). In contrast, *S. wolfei* ssp. *wolfei* is only known to β-oxidize fatty acids with four to eight
273 carbons (28). The different homologous β-oxidizing genes may also perform identical reactions
274 but have different kinetics and/or affinities, which could allow *S.* BUT1 to adapt to varying
275 substrate concentrations. This is supported by the detection of the *S.* BUT1 population in ^{13}C DNA
276 in the pulse-fed digester in the previous study by Ziels *et al.* (12), but not in the continuous-fed
277 digester in that study. Fluctuating environments are thought to lead to robustness towards gene
278 loss within metabolic networks through an increase in multifunctional enzymes (29). Thus, the
279 presence of various homologous genes for β-oxidation in *S.* BUT1 could have been selected for
280 by the fluctuating environmental conditions imposed from pulse-feeding the anaerobic digester. It
281 could also be possible that the *S.* BUT1 population was enriched in ^{13}C from labelled oleate due
282 to cross-feeding of shorter-chain intermediates during β-oxidation of the C_{18} LCFA, as other
283 syntrophic bacteria were enriched to a high degree during growth on labelled oleate (12). Yet, the
284 enrichment of *S.* BUT1 on ^{13}C-butyrate, along with the presence of the complete butyrate β-
285 oxidation pathway, strongly suggests that it is at least capable of β-oxidizing shorter chain fatty
286 acids (e.g. C_4) produced in anaerobic environments.
287

288 *Syntrophomonas* BUT1 lacks genes for aerobic or anaerobic respiration, which is similar to
289 genomes of *S. wolfei* and *Syntrophus aciditrophicus* that are capable of syntrophic butyrate
290 degradation (27, 30). Electrons derived from butyrate oxidation (reduced ETF from butyryl-CoA
291 oxidation and NADH from 3-hydroxybutyryl-CoA oxidation) must be disposed through reduction
292 of CO_2 to formate and H^+ to H_2 via formate dehydrogenases and hydrogenases respectively (31–
293 34). In the *S.* BUT1 genome, we identified genes encoding for butyryl-CoA dehydrogenase,
294 EtfAB, and two EtfAB:quinone oxidoreductases (Supplemental File 2), indicating that this
295 organism may transfer electrons from butyryl-CoA oxidation into membrane electron carriers
296 using ETF. The *S.* BUT1 genome contains five gene clusters encoding for formate
297 dehydrogenases, and four gene clusters encoding for hydrogenases (Supplemental File 2). These
298 included a membrane-bound cytochrome b-dependent selenocysteine-containing formate
299 dehydrogenase and [NiFe] hydrogenase that could receive butyrate-derived electrons via
300 menaquinol (31). The quinone-binding site of the selenocysteine-containing formate
301 dehydrogenase was on the cytoplasmic side, indicating that it likely utilizes proton motive force
302 to drive unfavorable electron transfer to CO_2-reducing formate generation outside of the cell.
303 Energy investment via "reverse electron transport" is critical to drive the uphill electron transfer
304 from butyryl-CoA/crotonyl-CoA couple to CO_2/formate or H^+/H_2 couples. In contrast, the quinone
305 binding site of the [NiFe] hydrogenase was on the periplasmic side, indicating it couples outward
306 vectorial proton transport with H_2 generation. Previous genomic and proteomic studies also
307 highlight the importance of ETF-based electron transfer, membrane-bound formate
308 dehydrogenases/hydrogenases, and reverse electron transport (6, 27, 34–37).
309

To complete syntrophic butyrate oxidation, NAD^+ must also be regenerated through oxidation of NADH. However, NADH oxidation coupled with CO_2/H^+-reducing formate/H_2 generation is thermodynamically unfavorable. To address this obstacle, anaerobic organisms are known to utilize electron bifurcation (or confurcation), which involves the coupling of endergonic and exergonic redox reactions to circumvent energetic barriers (38). For instance, *Thermotoga maritima* utilizes a trimeric hydrogenase to couple the endergonic production of H_2 from NADH with the exergonic production of H_2 from reduced ferredoxin (39). Two trimeric formate dehydrogenase- and two trimeric [FeFe]hydrogenase-encoding gene clusters in *S.* BUT1 appear linked to NADH, as they all contained a NADH:acceptor oxidoreductase subunit (Supplemental File 2). Yet, if the trimeric hydrogenases and formate dehydrogenases in *S.* BUT1 produce H_2/formate via electron bifurcation with NADH and ferredoxin, it remains unknown how *S.* BUT1 would regenerate reduced ferredoxin, as the known butyrate β-oxidation pathway does not generate reduced ferredoxin (31). Moreover, the *S.* BUT1 genome does not encode for a Rnf complex that would be necessary to generate reduced ferredoxin from NADH. Recently, the Fix (homologous to ETF) system was shown to perform electron-bifurcation to oxidize NADH coupled to the reduction of ferredoxin and ubiquinone during N_2 fixation by *Azotobacter vinelandii* (40). The *S.* BUT1 genome encoded for a Fix-related ETF-dehydrogenase, *fixC*, as well as its associated ferredoxin, *fixX* (Supplemental File 2). A Fix system has also been detected in *S. wolfei*, and was postulated to serve as a means of generating reduced ferredoxin for H_2 or formate production via the bifurcation mechanism (31). Yet, reduced ferredoxin production with the Fix system would be energetically costly, especially with regards to the low energy yields during syntrophic butyrate oxidation (41). Another mechanism was proposed for generating reduced ferredoxin in Rnf-lacking syntrophs that involves a heterodisulfide reductase complex (HdrABC)

and ion-translocating flavin oxidoreductase genes (Flx or Flox) (42). The *flxABCD-hdrABC* gene cluster was shown to be widespread among anaerobic bacteria, and the protein cluster (FlxABCD-HdrABC) is proposed to function similar to the HdrABC-MvhADG cluster involved in flavin based electron bifurcation in hydrogenotrophic methanogenic archaea that couples the exergonic reduction of CoM-S-S-CoB heterodisulfide with the endergonic reduction of ferredoxin with H_2 (43). A full *flxABCD-hdrABC* gene cluster was detected in the genome of *S.* BUT1 (Supplemental File 2). During the syntrophic growth of *S.* BUT1 on butyrate, the FlxABCD-HdrABC protein cluster could oxidize NADH with reduction of ferredoxin along with the reduction of a high-redox-potential disulfide acceptor (43). In *Desulfovibrio vulgaris*, it has been proposed that the DsrC serves as the high-redox thiol–disulfide electron carrier that is reduced by the FlxABCD-HdrABC complex during growth (44). The DsrC protein was also detected in the syntrophic benzoate-degrading *Syntrophorhabdus aromaticivorans* strain UI along with a *flxABCD-hdrABC* gene cluster (42), suggesting that the reduction of a thiol–disulfide electron carrier may be a conserved mechanism for generating reduced ferredoxin in syntrophic bacteria. Yet, the *S.* BUT1 genome does not encode for a DsrC protein, and thus an alternative and unknown thiol–disulfide electron carrier would be needed. Another possibility is that the trimeric hydrogenase can drive NADH-dependent H_2 generation as shown in *S. wolfei* Goettingen (41). Nonetheless, this genomic analysis demonstrates that *S.* BUT1 has the potential capacity to overcome energetic barriers during syntrophic butyrate β-oxidation, and contains multiple possible mechanisms for H_2 and formate production.

In addition to interspecies electron transfer via molecular hydrogen and formate, a potential mechanism has been proposed for direct interspecies electron transfer (DIET) in which electrons

356 are shared via electrically-conductive nanowires (45). DIET activity has been suggested in
357 enrichment communities degrading propionate and butyrate, in which *Syntrophomonas* was
358 detected (46, 47). However, DIET has not been demonstrated with pure cultures of
359 *Syntrophomonas* to date. The direct transfer of electrons is thought to depend on electrically
360 conductive type IV pili and external polyheme cytochromes (48, 49). The *S.* BUT1 genome
361 encodes for a type IV pilin assembly protein, *PilC*, but no genes were found that encoded for the
362 structural protein *PilA* that is associated with DIET (49). Moreover, the type IV pilin genes
363 identified in the *S.* BUT1 genome were of the type *Flp* (fimbrial low-molecular protein weight),
364 which are smaller than the *Pil* type pilin utilized for DIET in *Geobacter* (50, 51). A multiheme c-
365 type cytochrome was detected in the *S.* BUT1 genome that had 59% amino acid identity (89%
366 coverage) with the multiheme c-type cytochrome, OmcS, from *G. sulfurreducens* that has been
367 implicated in DIET (49) (Supplemental File 2). However, that gene also had higher homology
368 (69% identity, 94% coverage) with the cytochrome C nitrite reductase from *S. wolfei* (accession
369 no. WP_081424886). Therefore, the roles of DIET in the metabolism of *S.* BUT1 remain unclear,
370 but warrant further attention via expression-based profiling.
371
372 In addition to potential genetic mechanisms for energy conservation during syntrophic growth, *S.*
373 BUT1 also encoded for a capsule biosynthesis protein (*CapA*), which appears to be specific to
374 syntrophic growth (52). The function of *CapA* in syntrophic growth is unclear, but may be related
375 to the production of exopolymeric substances that facilitate interaction with methanogenic partners
376 (52). The *S.* BUT1 genome also encoded for the *FtsW* gene that is related to shape determination,
377 and is also a postulated biomarker of a syntrophic lifestyle (52). Based on the presence of these

'syntrophic biomarkers' along with genes for β-oxidization and H_2/formate production, the genomic repertoire of *S.* BUT1 aligns with that of a syntrophic butyrate degrader.

The genome of *S.* BUT1 was compared with published genomes of the *Syntrophomonas* genus (*S. wolfei* subsp. wolfei, *S. wolfei* subsp. methylbutyratica, and *S. zehnderi*) to investigate whether metabolic genes for beta-oxidation and energy conservation were conserved (Supplemental File S4). A cutoff of 42% amino acid similarity and 80% sequence overlap was employed based on the lowest first quartile amino acid similarity we observed for top blast hits (minimum of 20% amino acid similarity and 80% overlap) of *S.* BUT1 genes to each aforementioned *Syntrophomonas* genome (42.0%, 43.5%, and 43.5%, respectively). Based on these similarity thresholds, only 34% (1050 out of 3066) of protein-coding genes in the *S.* BUT1 genome have closely related homologs present in all of the other sequenced *Syntrophomonas* genomes. Notably, 40% of the *S.* BUT1 protein-coding genes have no homologs in other *Syntrophomonas* genomes that meet the similarity criteria above. Reflecting this genomic diversity, *S.* BUT1 encodes several beta oxidation-related genes that have no homologs in the other *Syntrophomonas* genomes that meet the above criteria: one acetyl-CoA acetyltransferase, acyl-CoA dehydrogenase, acrylyl-coa reductase, and acyl-CoA thioesterase (Supplemental File S4). In addition, the *S.* BUT1 genome harbors putative isobutyryl-CoA mutase genes (SYNMBUT1_v1_1780025 – 27) highly similar to those of *Syntrophothermus lipocalidus* (65.0-83.4% amino acid similarity), suggesting that *S.* BUT1 may also be capable of syntrophic isobutyrate degradation. Hydrogenases, formate dehydrogenases, and energy conservation genes were generally conserved among *S.* BUT1 and the other *Syntrophomonas* genomes. Only the cytochrome b-dependent [NiFe] hydrogenase has no homologs in the *S. wolfei* subsp. *wolfei* genome. This implies that *S.* BUT1 may have distinct capabilities for fatty acid

401 oxidation, but the energy conservation necessary to drive syntrophic beta oxidation may not vary
402 between *Syntrophomonas* species.
403
404 A genomic analysis of the *Methanothrix* BUT2 genome indicated that it contained the complete
405 pathway for methane production from acetate (Figure 4, Supplemental File 3). This observation
406 agrees with the physiology of other *Methanothrix* species, which are known aceticlastic
407 methanogens (53, 54). *M.* BUT2 also contained genes that likely are involved in energy
408 conservation during aceticlastic methanogenesis. The genome of *M.* BUT2 harbored acetyl-CoA
409 synthetase for acetate activation, bifunctional CO dehydrogenase/acetyl-CoA synthase
410 (CODH/ACS) to oxidatively split acetyl-CoA into CO_2 and CH_3-H_4MPT,
411 tetrahydromethanopterin S-methyltransferase, and methyl-CoM reductase for methyl-CoM
412 reduction to CH_4 (Supplemental File 3). To couple acetyl-CoA oxidation and reductive CH_4
413 generation, BUT2 must transfer electrons from Fd_{red} to CoM-SH/CoB-SH. We identified a FpoF-
414 lacking $F_{420}H_2$ dehydrogenase (Fpo) complex and heterodisulfide reductase (HdrDE) that could
415 facilitate this (Supplemental File 3) and also generate an ion motive force (55). This energy
416 conservation system is highly similar to *M. thermophila* acetate oxidation (55). In previous studies,
417 *Methanothrix* species have been observed to co-occur with *Syntrophomonas* in LCFA-degrading
418 (56) and butyrate-degrading (57–59) anaerobic environments. In this study, the stable isotope-
419 informed metagenomic analysis strongly suggests that the labelling of *M.* BUT2 DNA was due to
420 the incorporation of ^{13}C-acetate produced during the degradation of ^{13}C-butyrate by *S.* BUT1.
421
422 A near-complete pathway for methane production from CO_2 was also observed in the *M.* BUT2
423 genome (Supplemental File 3). The only gene lacking in the CO_2-reducing pathway was a F_{420}-

424 dependent N_5N_{10}-methylene-tetrahydromethanopterin dehydrogenase (Mtd). While *Methanothrix*
425 are thought to be obligate aceticlastic methanogens (53, 54), the presence and expression of the
426 CO_2-reducing pathway in *Methanothrix* was previously reported (60–62) and was hypothesized to
427 be involved in methane formation via DIET. However, the mechanism through which
428 *Methanothrix* would directly accept electrons from its syntrophic partner has not been identified
429 (60, 61). The other known electron donors for methane production from CO_2 are hydrogen and
430 formate. A membrane bound hydrogenase (*mbhAB*) was observed in the *M.* BUT2 genome
431 (Supplemental File 3). In other studies, negligible hydrogenase activity was observed with
432 *Methanothrix* species (63). Two monomeric formate dehydrogenase enzymes (*fdhA*) were also
433 encoded in *M.* BUT2 (Supplemental File 3). Experiments with thermophilic *M.* sp. strain CALS-
434 1 and mesophilic *M. concilii* showed that they displayed formate dehydrogenase activity by
435 splitting formate into hydrogen and CO_2, however the produced CO_2 was not used for methane
436 generation (63, 64). Yet, the mesophilic *M. soehngenii* did not show formate dehydrogenase
437 activity (54). Thus, the roles of the hydrogenases, formate dehydrogenases, and CO_2-reducing
438 pathway for methane generation in *M.* BUT2 are not clear. Transcriptomic or proteomic
439 approaches are needed to elucidate the activity of the CO_2-reducing methanogenesis production
440 pathway during syntrophic growth on butyrate with *S.* BUT1.
441
442 **Conclusions**
443 In this study, stable isotope-informed genome-resolved metagenomics was used to provide
444 genomic insight into syntrophic metabolism during butyrate degradation in anaerobic digesters.
445 The results obtained via genome binning and metabolic reconstruction showed that the ^{13}C-
446 enriched *Syntrophomonas* genome contained the genetic capacity to convert butyrate into

447 precursor metabolites for methane formation—acetate, hydrogen and formate. The ^{13}C-enriched
448 *Methanothrix* genome likely consumed the acetate produced during butyrate degradation,
449 incorporating some ^{13}C into biomass. The presence of a CO_2-reducing pathway, as well as formate
450 dehydrogenase and hydrogenase genes, in the *Methanothrix* genome leaves open the possibility of
451 flexible metabolism during methanogenesis. As syntrophic fatty acid degrading populations are
452 often slow-growing and thus difficult to isolate, this study demonstrates a new approach to link
453 ecophysiology with genomic identity in these important populations involved in anaerobic
454 biotechnologies, as well as global carbon cycling. Advancing our understanding of *in-situ*
455 metabolic activities within anaerobic communities is paramount, as these microbiomes contain
456 multiple interacting functional groups that, in cooperation, enable the processing of degradable
457 organic carbon into methane gas. Coupling SIP-informed metagenomics with other activity-based
458 techniques, such as metabolomics, transcriptomics, and proteomics, could further illuminate the
459 structure of anaerobic metabolic networks as well as quantify metabolite fluxes, thus enabling
460 newly informed process models to predict rates of anaerobic carbon transformation.
461

Experimental Procedures

Batch incubations with ^{13}C-labelled butyrate

Two 4 L anaerobic digesters treating dairy manure and sodium oleate were operated for over 200 d at a solids retention time of 20 d and a temperature of 35°C, as described by Ziels *et al.* (56). The two digesters were operated with different feeding frequencies of sodium oleate. One digester received sodium oleate once every 48 hrs, while the other digester was fed semi-continuously every 6 hrs (56).

On day 228 of digester operation, 10 mL samples were collected from each digester, and immediately transferred to 35 mL glass serum bottles that were pre-purged with N_2:CO_2 (80:20), and capped with butyl rubber septa. Duplicate microcosms were fed with a 1 M solution of either ^{12}C sodium butyrate or ^{13}C-labeled sodium butyrate (>98% atom purity, Cambridge Isotope Laboratories, Tewksbury, MA, USA) to reach an initial butyrate concentration of 40 mM. The ^{13}C-labeled sodium butyrate was universally labeled at all 4 carbons. Triplicate blank controls were incubated in parallel to measure background methane production from the inoculum. Methane production was measured approximately every 4 hr over the 50 hr incubation time using a digital manometer (Series 490 A, Dwyer Instruments) and GC-FID (SRI 8610C), according to Ziels *et al.* (56).

Stable isotope probing

DNA was extracted from the duplicate 10 mL microcosms after the 50-hr incubation, and was separated via density-gradient centrifugation and fractionated as previously described (12). DNA was measured in 24 density gradient fractions using QuBit (Invitrogen, MA, USA).

485 *Syntrophomonas* 16S rRNA genes were quantified in gradient fractions as described by Ziels et al.
486 (12), using previously developed primers and probes (65). Heavy DNA fractions with buoyant
487 densities between 1.70-1.705 g/mL (Supplemental Figure S2) were selected for each microcosm
488 sample and sent for metagenomic sequencing at MR DNA Laboratories (Shallowater, TX, USA),
489 as well as for 16S rRNA gene iTag sequencing at the U.S. Department of Energy Joint Genome
490 Institute (JGI) according to Ziels *et al.* (12). Metagenome libraries were prepared using the Nextera
491 DNA sample preparation kit (Illumina Inc., Hayward, CA, USA) following the manufacturer's
492 instructions. The metagenome libraries were sequenced in 150 bp paired-end mode on a HiSeq
493 2500 (Illumina Inc., Hayward, California, USA). Bioinformatic analysis of the 16S rRNA iTags
494 is described in detail in the Supporting Information.
495
496 *Genome binning, annotation, and statistical analysis*
497 All metagenomic reads were initially trimmed and quality filtered using illumina-utils (66)
498 (available from: https://github.com/merenlab/illumina-utils) according to the parameters of
499 Minoche et al. (67). Metagenomic reads from all ^{13}C-butyrate fed microcosms were co-assembled
500 using MEGAHIT v1.1.1 (68). Open reading frames were called with Prodigal v.2.6.3 (69), and
501 were taxonomically classified with GhostKOALA (70). Short reads from the ^{12}C and ^{13}C
502 metagenomes were mapped onto the contigs using Bowtie2 (71) with default parameters.
503 Additionally, metagenomic reads from the total biomass collected from each digester 2 days after
504 the butyrate SIP experiment (i.e. time zero) (12) were mapped onto the assembled contigs to
505 facilitate the subsequent differential coverage binning. The contigs were then binned according to
506 the workflow of Eren *et al.* (72) using Anvi'o v.2.4.0, as described in detail in the Supplemental
507 Information. After manual refinement of the bins using Anvi'o, we obtained a set of 160 genomic

bins that were assessed for completeness and contamination with CheckM (72) (Supplemental File 1). Differential abundance of each genomic bin in the ^{13}C and ^{12}C butyrate metagenomes of each digester was determined using DESeq2 (14) using mapped read counts. A significant difference in abundance between ^{12}C and ^{13}C metagenomes was established by a *p* value less than 0.05. The average nucleotide identity (ANI) between ^{13}C-enriched genomic bins and publicly-available genomes from closely-related organisms were calculated with pyANI (available from: https://github.com/widdowquinn/pyani). Open reading frames were annotated with the MicroScope platform (73), and metabolic reconstructions were performed in Pathway Tools (74). Potential type IV pilin genes were identified with the PilFind program (50).

Data Availability

We have made publicly available the following: raw sequence reads and metagenome assemblies for the butyrate DNA-SIP metagenomes under NCBI Sequence Read Archive under BioProject PRJNA524401; genomic FASTA files for each ^{13}C-enriched genomic bin (https://doi.org/10.6084/m9.figshare.7761776); and the annotation data for the two ^{13}C enriched MAGs (https://doi.org/10.6084/m9.figshare.7761710). The time-zero raw metagenomic reads from the study by Ziels et al. (12) that were used for differential coverage binning, are available via the U.S. Joint Genome Institute Genome Portal (https://genome.jgi.doe.gov/portal/) under Project IDs: 1105507, 1105497. 16S rRNA gene amplicon sequences are available via the U.S. Joint Genome Institute Genome Portal under Project Number: 1105527, Sample IDs: 112232-112239.

Acknowledgments

This work was funded by US EPA STAR [grant RD835567] and ERC [grant 323009]. The work conducted by the U.S. Department of Energy Joint Genome Institute, a DOE Office of Science User Facility, is supported by the Office of Science of the U.S. Department of Energy under Contract No. DE-AC02-05CH11231.

We acknowledge H. David Stensel and Alfons Stams for their helpful input.

538
539 **References:**

540 1. Neufeld JD, Wagner M, Murrell JC. 2007. Who eats what, where and when? Isotope-
541 labelling experiments are coming of age. ISME J 1:103–110.

542 2. Batstone DJ, Virdis B. 2014. The role of anaerobic digestion in the emerging energy
543 economy. Current Opinion in Biotechnology 27:142–149.

544 3. Briones A, Raskin L. 2003. Diversity and dynamics of microbial communities in
545 engineered environments and their implications for process stability. Current Opinion in
546 Biotechnology 14:270–276.

547 4. Vanwonterghem I, Jensen PD, Rabaey K, Tyson GW. 2016. Genome-centric resolution of
548 microbial diversity, metabolism and interactions in anaerobic digestion. Environmental
549 Microbiology 18:3144–3158.

550 5. McInerney MJ, Struchtemeyer CG, Sieber J, Mouttaki H, Stams AJM, Schink B, Rohlin L,
551 Gunsalus RP. 2008. Physiology, Ecology, Phylogeny, and Genomics of Microorganisms
552 Capable of Syntrophic Metabolism. Annals of the New York Academy of Sciences
553 1125:58–72.

554 6. Schink B. 1997. Energetics of syntrophic cooperation in methanogenic degradation.
555 Microbiol Mol Biol Rev 61:262–280.

556 7. Sousa DZ, Smidt H, Alves MM, Stams AJM. 2009. Ecophysiology of syntrophic
557 communities that degrade saturated and unsaturated long-chain fatty acids. FEMS
558 Microbiol Ecol 68:257–272.

559 8. Narihiro T, Terada T, Ohashi A, Kamagata Y, Nakamura K, Sekiguchi Y. 2012.
560 Quantitative detection of previously characterized syntrophic bacteria in anaerobic
561 wastewater treatment systems by sequence-specific rRNA cleavage method. Water
562 Research 46:2167–2175.

563 9. Ahring BK, Westermann P. 1987. Kinetics of Butyrate, Acetate, and Hydrogen Metabolism
564 in a Thermophilic, Anaerobic, Butyrate-Degrading Triculture. Appl Environ Microbiol
565 53:434–439.

566 10. Hatamoto M, Imachi H, Yashiro Y, Ohashi A, Harada H. 2008. Detection of Active
567 Butyrate-Degrading Microorganisms in Methanogenic Sludges by RNA-Based Stable
568 Isotope Probing. Appl Environ Microbiol 74:3610–3614.

569 11. Treu L, Kougias PG, Campanaro S, Bassani I, Angelidaki I. 2016. Deeper insight into the
570 structure of the anaerobic digestion microbial community; the biogas microbiome database
571 is expanded with 157 new genomes. Bioresource Technology 216:260–266.

572 12. Ziels RM, Sousa DZ, Stensel HD, Beck DAC. 2018. DNA-SIP based genome-centric
573 metagenomics identifies key long-chain fatty acid-degrading populations in anaerobic
574 digesters with different feeding frequencies. The ISME Journal 12:112–123.

575 13. Neufeld JD, Vohra J, Dumont MG, Lueders T, Manefield M, Friedrich MW, Murrell JC.
576 2007. DNA stable-isotope probing. Nat Protocols 2:860–866.

577 14. Love MI, Huber W, Anders S. 2014. Moderated estimation of fold change and dispersion
578 for RNA-seq data with DESeq2. Genome Biology 15:550.

579 15. Ariesyady HD, Ito T, Okabe S. 2007. Functional bacterial and archaeal community
580 structures of major trophic groups in a full-scale anaerobic sludge digester. Water Research
581 41:1554–1568.

582 16. Liu P, Qiu Q, Lu Y. 2011. Syntrophomonadaceae-affiliated species as active butyrate-
583 utilizing syntrophs in paddy field soil. Appl Environ Microbiol.

584 17. Westerholm M, Roos S, Schnürer A. 2011. Tepidanaerobacter acetatoxydans sp. nov., an
585 anaerobic, syntrophic acetate-oxidizing bacterium isolated from two ammonium-enriched
586 mesophilic methanogenic processes. Systematic and Applied Microbiology 34:260–266.

587 18. McIlroy SJ, Kirkegaard RH, Dueholm MS, Fernando E, Karst SM, Albertsen M, Nielsen
588 PH. 2017. Culture-Independent Analyses Reveal Novel Anaerolineaceae as Abundant
589 Primary Fermenters in Anaerobic Digesters Treating Waste Activated Sludge. Front
590 Microbiol 8.

591 19. Bowers RM, Kyrpides NC, Stepanauskas R, Harmon-Smith M, Doud D, Reddy TBK,
592 Schulz F, Jarett J, Rivers AR, Eloe-Fadrosh EA, Tringe SG, Ivanova NN, Copeland A,
593 Clum A, Becraft ED, Malmstrom RR, Birren B, Podar M, Bork P, Weinstock GM, Garrity
594 GM, Dodsworth JA, Yooseph S, Sutton G, Glöckner FO, Gilbert JA, Nelson WC, Hallam
595 SJ, Jungbluth SP, Ettema TJG, Tighe S, Konstantinidis KT, Liu W-T, Baker BJ, Rattei T,
596 Eisen JA, Hedlund B, McMahon KD, Fierer N, Knight R, Finn R, Cochrane G, Karsch-
597 Mizrachi I, Tyson GW, Rinke C, Consortium TGS, Kyrpides NC, Schriml L, Garrity GM,
598 Hugenholtz P, Sutton G, Yilmaz P, Meyer F, Glöckner FO, Gilbert JA, Knight R, Finn R,
599 Cochrane G, Karsch-Mizrachi I, Lapidus A, Meyer F, Yilmaz P, Parks DH, Eren AM,
600 Schriml L, Banfield JF, Hugenholtz P, Woyke T. 2017. Minimum information about a
601 single amplified genome (MISAG) and a metagenome-assembled genome (MIMAG) of
602 bacteria and archaea. Nature Biotechnology 35:nbt.3893.

603 20. Parks DH, Imelfort M, Skennerton CT, Hugenholtz P, Tyson GW. 2015. CheckM:
604 assessing the quality of microbial genomes recovered from isolates, single cells, and
605 metagenomes. Genome Res gr.186072.114.

606 21. Caro-Quintero A, Konstantinidis KT. 2012. Bacterial species may exist, metagenomics
607 reveal. Environmental Microbiology 14:347–355.

608 22. Sousa DZ, Smidt H, Alves MM, Stams AJM. 2007. Syntrophomonas zehnderi sp. nov., an
609 anaerobe that degrades long-chain fatty acids in co-culture with Methanobacterium

formicicum. International Journal of Systematic and Evolutionary Microbiology 57:609–615.

23. Goris J, Konstantinidis KT, Klappenbach JA, Coenye T, Vandamme P, Tiedje JM. 2007. DNA–DNA hybridization values and their relationship to whole-genome sequence similarities. International Journal of Systematic and Evolutionary Microbiology 57:81–91.

24. Palatsi J, Illa J, Prenafeta-Boldú FX, Laureni M, Fernandez B, Angelidaki I, Flotats X. 2010. Long-chain fatty acids inhibition and adaptation process in anaerobic thermophilic digestion: Batch tests, microbial community structure and mathematical modelling. Bioresource Technology 101:2243–2251.

25. Parks DH, Rinke C, Chuvochina M, Chaumeil P-A, Woodcroft BJ, Evans PN, Hugenholtz P, Tyson GW. 2017. Recovery of nearly 8,000 metagenome-assembled genomes substantially expands the tree of life. Nature Microbiology 2:1533–1542.

26. Kleerebezem R, Loosdrecht MCMV. 2010. A Generalized Method for Thermodynamic State Analysis of Environmental Systems. Critical Reviews in Environmental Science and Technology 40:1–54.

27. Sieber JR, McInerney MJ, Gunsalus RP. 2012. Genomic Insights into Syntrophy: The Paradigm for Anaerobic Metabolic Cooperation. http://dx.doi.org/101146/annurev-micro-090110-102844. review-article.

28. McInerney MJ, Bryant MP, Pfennig N. 1979. Anaerobic bacterium that degrades fatty acids in syntrophic association with methanogens. Arch Microbiol 122:129–135.

29. Soyer OS, Pfeiffer T. 2010. Evolution under Fluctuating Environments Explains Observed Robustness in Metabolic Networks. PLOS Computational Biology 6:e1000907.

30. McInerney MJ, Rohlin L, Mouttaki H, Kim U, Krupp RS, Rios-Hernandez L, Sieber J, Struchtemeyer CG, Bhattacharyya A, Campbell JW, Gunsalus RP. 2007. The genome of Syntrophus aciditrophicus: Life at the thermodynamic limit of microbial growth. PNAS 104:7600–7605.

31. Sieber JR, Sims DR, Han C, Kim E, Lykidis A, Lapidus AL, McDonnald E, Rohlin L, Culley DE, Gunsalus R, McInerney MJ. 2010. The genome of Syntrophomonas wolfei: new insights into syntrophic metabolism and biohydrogen production. Environmental Microbiology 12:2289–2301.

32. Sieber JR, Le HM, McInerney MJ. 2014. The importance of hydrogen and formate transfer for syntrophic fatty, aromatic and alicyclic metabolism. Environmental Microbiology 16:177–188.

33. Sieber JR, Crable BR, Sheik CS, Hurst GB, Rohlin L, Gunsalus RP, McInerney MJ. 2015. Proteomic analysis reveals metabolic and regulatory systems involved in the syntrophic and axenic lifestyle of Syntrophomonas wolfei. Front Microbiol 6.

646 34. Schmidt A, Müller N, Schink B, Schleheck D. 2013. A Proteomic View at the Biochemistry
647 of Syntrophic Butyrate Oxidation in Syntrophomonas wolfei. PLOS ONE 8:e56905.

648 35. Crable BR, Sieber JR, Mao X, Alvarez-Cohen L, Gunsalus R, Loo O, R R, Nguyen H,
649 McInerney MJ. 2016. Membrane Complexes of Syntrophomonas wolfei Involved in
650 Syntrophic Butyrate Degradation and Hydrogen Formation. Front Microbiol 7.

651 36. Müller N, Schleheck D, Schink B. 2009. Involvement of NADH:Acceptor Oxidoreductase
652 and Butyryl Coenzyme A Dehydrogenase in Reversed Electron Transport during
653 Syntrophic Butyrate Oxidation by Syntrophomonas wolfei. J Bacteriol 191:6167–6177.

654 37. Wallrabenstein C, Schink B. 1994. Evidence of reversed electron transport in syntrophic
655 butyrate or benzoate oxidation by Syntrophomonas wolfei and Syntrophus buswellii. Arch
656 Microbiol 162:136–142.

657 38. Buckel W, Thauer RK. 2018. Flavin-Based Electron Bifurcation, Ferredoxin, Flavodoxin,
658 and Anaerobic Respiration With Protons (Ech) or NAD+ (Rnf) as Electron Acceptors: A
659 Historical Review. Front Microbiol 9.

660 39. Schut GJ, Adams MWW. 2009. The Iron-Hydrogenase of Thermotoga maritima Utilizes
661 Ferredoxin and NADH Synergistically: a New Perspective on Anaerobic Hydrogen
662 Production. J Bacteriol 191:4451–4457.

663 40. Ledbetter RN, Garcia Costas AM, Lubner CE, Mulder DW, Tokmina-Lukaszewska M,
664 Artz JH, Patterson A, Magnuson TS, Jay ZJ, Duan HD, Miller J, Plunkett MH, Hoben JP,
665 Barney BM, Carlson RP, Miller A-F, Bothner B, King PW, Peters JW, Seefeldt LC. 2017.
666 The Electron Bifurcating FixABCX Protein Complex from Azotobacter vinelandii:
667 Generation of Low-Potential Reducing Equivalents for Nitrogenase Catalysis. Biochemistry
668 56:4177–4190.

669 41. Losey NA, Mus F, Peters JW, Le HM, McInerney MJ. 2017. Syntrophomonas wolfei Uses
670 an NADH-Dependent, Ferredoxin-Independent [FeFe]-Hydrogenase To Reoxidize NADH.
671 Appl Environ Microbiol 83:e01335-17.

672 42. Nobu MK, Narihiro T, Hideyuki T, Qiu Y-L, Sekiguchi Y, Woyke T, Goodwin L,
673 Davenport KW, Kamagata Y, Liu W-T. 2015. The genome of Syntrophorhabdus
674 aromaticivorans strain UI provides new insights for syntrophic aromatic compound
675 metabolism and electron flow. Environmental Microbiology 17:4861–4872.

676 43. Ramos AR, Grein F, Oliveira GP, Venceslau SS, Keller KL, Wall JD, Pereira IAC. 2015.
677 The FlxABCD-HdrABC proteins correspond to a novel NADH
678 dehydrogenase/heterodisulfide reductase widespread in anaerobic bacteria and involved in
679 ethanol metabolism in Desulfovibrio vulgaris Hildenborough. Environmental Microbiology
680 17:2288–2305.

681 44. Meyer B, Kuehl J, Deutschbauer AM, Price MN, Arkin AP, Stahl DA. 2013. Variation
682 among Desulfovibrio Species in Electron Transfer Systems Used for Syntrophic Growth.
683 Journal of Bacteriology 195:990–1004.

684 45. Reguera G, McCarthy KD, Mehta T, Nicoll JS, Tuominen MT, Lovley DR. 2005.
685 Extracellular electron transfer via microbial nanowires. Nature 435:1098–1101.

686 46. Zhao Z, Li Y, Yu Q, Zhang Y. 2018. Ferroferric oxide triggered possible direct interspecies
687 electron transfer between Syntrophomonas and Methanosaeta to enhance waste activated
688 sludge anaerobic digestion. Bioresource Technology 250:79–85.

689 47. Zhao Z, Zhang Y, Yu Q, Dang Y, Li Y, Quan X. 2016. Communities stimulated with
690 ethanol to perform direct interspecies electron transfer for syntrophic metabolism of
691 propionate and butyrate. Water Research 102:475–484.

692 48. Malvankar NS, Lovley DR. 2014. Microbial nanowires for bioenergy applications. Current
693 Opinion in Biotechnology 27:88–95.

694 49. Summers ZM, Fogarty HE, Leang C, Franks AE, Malvankar NS, Lovley DR. 2010. Direct
695 Exchange of Electrons Within Aggregates of an Evolved Syntrophic Coculture of
696 Anaerobic Bacteria. Science 330:1413–1415.

697 50. Imam S, Chen Z, Roos DS, Pohlschröder M. 2011. Identification of Surprisingly Diverse
698 Type IV Pili, across a Broad Range of Gram-Positive Bacteria. PLOS ONE 6:e28919.

699 51. Walker DJ, Nevin KP, Holmes DE, Rotaru A-E, Ward JE, Woodard TL, Zhu J, Ueki T,
700 Nonnenmann SS, McInerney MJ, Lovley DR. 2018. Syntrophus Conductive Pili
701 Demonstrate that Common Hydrogen-Donating Syntrophs can have a Direct Electron
702 Transfer Option. bioRxiv 479683.

703 52. Worm P, Koehorst JJ, Visser M, Sedano-Núñez VT, Schaap PJ, Plugge CM, Sousa DZ,
704 Stams AJM. 2014. A genomic view on syntrophic versus non-syntrophic lifestyle in
705 anaerobic fatty acid degrading communities. Biochimica et Biophysica Acta (BBA) -
706 Bioenergetics 1837:2004–2016.

707 53. Huser BA, Wuhrmann K, Zehnder AJB. 1982. Methanothrix soehngenii gen. nov. sp. nov.,
708 a new acetotrophic non-hydrogen-oxidizing methane bacterium. Arch Microbiol 132:1–9.

709 54. Touzel JP, Prensier G, Roustan JL, Thomas I, Dubourguier HC, Albagnac G. 1988.
710 Description of a New Strain of Methanothrix soehngenii and Rejection of Methanothrix
711 concilii as a Synonym of Methanothrix soehngenii. International Journal of Systematic and
712 Evolutionary Microbiology 38:30–36.

713 55. Welte C, Deppenmeier U. 2011. Membrane-Bound Electron Transport in Methanosaeta
714 thermophila. Journal of Bacteriology 193:2868–2870.

715 56. Ziels RM, Beck DAC, Stensel HD. 2017. Long-chain fatty acid feeding frequency in
716 anaerobic codigestion impacts syntrophic community structure and biokinetics. Water
717 Research 117:218–229.

718 57. Tang Y-Q, Shigematsu T, Morimura S, Kida K. 2007. Effect of dilution rate on the
719 microbial structure of a mesophilic butyrate-degrading methanogenic community during
720 continuous cultivation. Appl Microbiol Biotechnol 75:451–465.

721 58. Schmidt O, Hink L, Horn MA, Drake HL. 2016. Peat: home to novel syntrophic species
722 that feed acetate- and hydrogen-scavenging methanogens. The ISME Journal 10:1954–
723 1966.

724 59. Chauhan A, Ogram A. 2006. Fatty Acid-Oxidizing Consortia along a Nutrient Gradient in
725 the Florida Everglades. Appl Environ Microbiol 72:2400–2406.

726 60. Holmes DE, Shrestha PM, Walker DJF, Dang Y, Nevin KP, Woodard TL, Lovley DR.
727 2017. Metatranscriptomic Evidence for Direct Interspecies Electron Transfer between
728 Geobacter and Methanothrix Species in Methanogenic Rice Paddy Soils. Appl Environ
729 Microbiol 83:e00223-17.

730 61. Rotaru A-E, Malla Shrestha P, Liu F, Shrestha M, Shrestha D, Embree M, Zengler K,
731 Wardman C, P. Nevin K, R. Lovley D. 2014. A new model for electron flow during
732 anaerobic digestion: direct interspecies electron transfer to Methanosaeta for the reduction
733 of carbon dioxide to methane. Energy & Environmental Science 7:408–415.

734 62. Zhu J, Zheng H, Ai G, Zhang G, Liu D, Liu X, Dong X. 2012. The Genome Characteristics
735 and Predicted Function of Methyl-Group Oxidation Pathway in the Obligate Aceticlastic
736 Methanogens, Methanosaeta spp. PLOS ONE 7:e36756.

737 63. Zinder SH, Anguish T. 1992. Carbon Monoxide, Hydrogen, and Formate Metabolism
738 during Methanogenesis from Acetate by Thermophilic Cultures of Methanosarcina and
739 Methanothrix Strains. Appl Environ Microbiol 58:3323–3329.

740 64. Patel GB. 1984. Characterization and nutritional properties of Methanothrix concilii sp.
741 nov., a mesophilic, aceticlastic methanogen. Can J Microbiol 30:1383–1396.

742 65. Ziels RM, Beck DAC, Martí M, Gough HL, Stensel HD, Svensson BH. 2015. Monitoring
743 the dynamics of syntrophic β-oxidizing bacteria during anaerobic degradation of oleic acid
744 by quantitative PCR. FEMS Microbiol Ecol 91.

745 66. Eren AM, Vineis JH, Morrison HG, Sogin ML. 2013. A Filtering Method to Generate High
746 Quality Short Reads Using Illumina Paired-End Technology. PLOS ONE 8:e66643.

747 67. Minoche AE, Dohm JC, Himmelbauer H. 2011. Evaluation of genomic high-throughput
748 sequencing data generated on Illumina HiSeq and Genome Analyzer systems. Genome
749 Biology 12:R112.

750 68. Li D, Luo R, Liu C-M, Leung C-M, Ting H-F, Sadakane K, Yamashita H, Lam T-W. 2016.
751 MEGAHIT v1.0: A fast and scalable metagenome assembler driven by advanced
752 methodologies and community practices. Methods 102:3–11.

753 69. Hyatt D, Chen G-L, LoCascio PF, Land ML, Larimer FW, Hauser LJ. 2010. Prodigal:
754 prokaryotic gene recognition and translation initiation site identification. BMC
755 Bioinformatics 11:119.

756 70. Kanehisa M, Sato Y, Morishima K. 2016. BlastKOALA and GhostKOALA: KEGG Tools
757 for Functional Characterization of Genome and Metagenome Sequences. Journal of
758 Molecular Biology 428:726–731.

759 71. Langmead B, Salzberg SL. 2012. Fast gapped-read alignment with Bowtie 2. Nature
760 Methods 9:357–359.

761 72. Eren AM, Esen ÖC, Quince C, Vineis JH, Morrison HG, Sogin ML, Delmont TO. 2015.
762 Anvi'o: an advanced analysis and visualization platform for 'omics data. PeerJ 3:e1319.

763 73. Vallenet D, Belda E, Calteau A, Cruveiller S, Engelen S, Lajus A, Le Fèvre F, Longin C,
764 Mornico D, Roche D, Rouy Z, Salvignol G, Scarpelli C, Thil Smith AA, Weiman M,
765 Médigue C. 2013. MicroScope—an integrated microbial resource for the curation and
766 comparative analysis of genomic and metabolic data. Nucleic Acids Res 41:D636–D647.

767 74. Karp PD, Paley SM, Krummenacker M, Latendresse M, Dale JM, Lee TJ, Kaipa P, Gilham
768 F, Spaulding A, Popescu L, Altman T, Paulsen I, Keseler IM, Caspi R. 2010. Pathway
769 Tools version 13.0: integrated software for pathway/genome informatics and systems
770 biology. Brief Bioinform 11:40–79.

771 75. Campbell JH, O'Donoghue P, Campbell AG, Schwientek P, Sczyrba A, Woyke T, Söll D,
772 Podar M. 2013. UGA is an additional glycine codon in uncultured SR1 bacteria from the
773 human microbiota. PNAS 110:5540–5545.

774 76. Finn RD, Clements J, Eddy SR. 2011. HMMER web server: interactive sequence similarity
775 searching. Nucleic Acids Res 39:W29–W37.

776 77. Price MN, Dehal PS, Arkin AP. 2009. FastTree: Computing Large Minimum Evolution
777 Trees with Profiles instead of a Distance Matrix. Mol Biol Evol 26:1641–1650.

778 78. Rinke C, Schwientek P, Sczyrba A, Ivanova NN, Anderson IJ, Cheng J-F, Darling A,
779 Malfatti S, Swan BK, Gies EA, Dodsworth JA, Hedlund BP, Tsiamis G, Sievert SM, Liu
780 W-T, Eisen JA, Hallam SJ, Kyrpides NC, Stepanauskas R, Rubin EM, Hugenholtz P,
781 Woyke T. 2013. Insights into the phylogeny and coding potential of microbial dark matter.
782 Nature 499:431–437.

783
784
785
786
787
788
789

Table 1: Genomic feature summary of the two metagenome-assembled genomes that were significantly enriched in ^{13}C after the degradation of labeled butyrate.

Name	Bin ID	Taxonomy[1]	Size (Mb)	GC (%)	Completion (%)[2]	Redundancy (%)[2]	Quality Classification[3]
Syntrophomonas BUT1	Bin 26_1	*Syntrophomonas*	2.87	51.2	96.4	1.4	High Quality Draft
Methanothrix BUT2	Bin 26_2	*Methanothrix*	1.44	53.6	74.7	3.1	Medium Quality Draft

[1] Based on phylogenetic placement of single marker genes with CheckM (72)
[2] Measured with Anvi'o (72)
[3] Based on parameters suggested by Bowers *et al.* (19)

Table 2: Gibbs free energy for some of the acetogenic and methanogenic reactions likely involved in the syntrophic conversion of butyrate and oleate.

Reaction	$\Delta_r G'°$	$\Delta_r G'$ [1]
Acetogenic Reactions		
$Butyrate^- + 2\ H_2O \rightleftharpoons 2\ Acetate^- + 2\ H_{2(g)} + H^+$	+53.1 ± 13.6	-21.1 ± 13.6
$Oleate^- + 16\ H_2O \rightleftharpoons 9\ acetate^- + 15\ H_{2(g)} + 8H^+$	+344.9 ± 91.5	-219.9 ± 91.5
Methanogenic Reactions (Butyrate oxidation) [2]		
$2\ H_{2(g)} + 1/2\ CO_{2(g)} \rightleftharpoons 1/2\ CH_{4(g)} + H_2O$	-66.5 ± 12.4	-9.4 ± 12.4
$2\ Acetate^- + 2\ H^+ \rightleftharpoons 2\ CO_{2(g)} + 2\ CH_{4(g)}$	-70.3 ± 16.9	-58.9 ± 16.9
Methanogenic Reactions (Oleate oxidation) [2]		
$15\ H_{2(g)} + 15/4\ CO_{2(g)} \rightleftharpoons 15/4\ CH_{4(g)} + 15/2\ H_2O$	-498.5 ± 93.0	-70.6 ± 93.0
$9\ Acetate^- + 9\ H^+ \rightleftharpoons 9\ CO_{2(g)} + 9\ CH_{4(g)}$	-316.3 ± 75.9	-264.9 ± 75.9
Overall Reactions		
$Butyrate^- + H_2O + H^+ \rightleftharpoons 3/2\ CO_{2(g)} + 5/2\ CH_{4(g)}$	-83.7 ± 18.0	-89.4 ± 18.0
$Oleate^- + 17/2\ H_2O + H^+ \rightleftharpoons 51/4\ CH_{4(g)} + 21/4\ CO_{2(g)}$	-469.8 ± 81.9	-555.4 ± 81.9

[1] All values are in units of kJ/mole-reaction, and were calculated using eQuilibrator (http://equilibrator.weizmann.ac.il/) at 25°C, pH of 7 and ionic strength of 1. $\Delta_r G'$ values were calculated based on fatty acid concentrations of 1 mM, H_2 partial pressures of 1 Pa, and CO_2 and CH_4 partial pressures of 10^4 Pa.
[2] The stoichiometry of the methanogenic reactions were scaled proportionally to consume the products from oxidizing 1 mole of fatty acid.

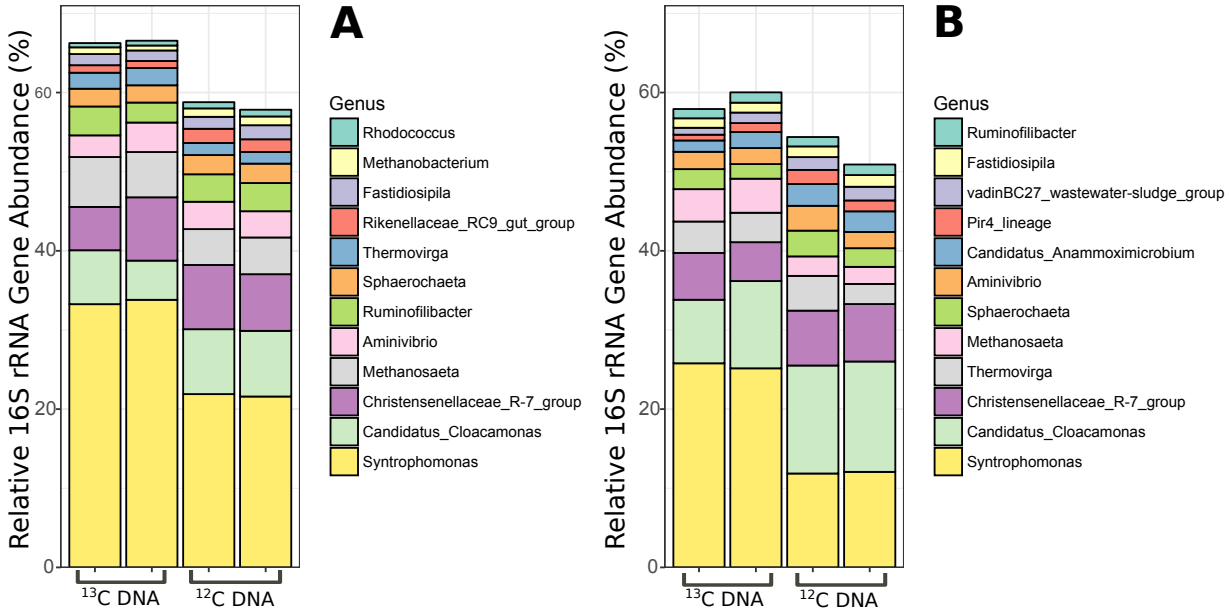

Figure 1: Relative 16S rRNA gene amplicon sequence abundance of the top 12 most abundant prokaryotic genera in the ^{13}C butyrate-amended microcosms and the ^{12}C butyrate-amended controls for (A) the pulse-fed codigester and (B) the continuous-fed codigester.

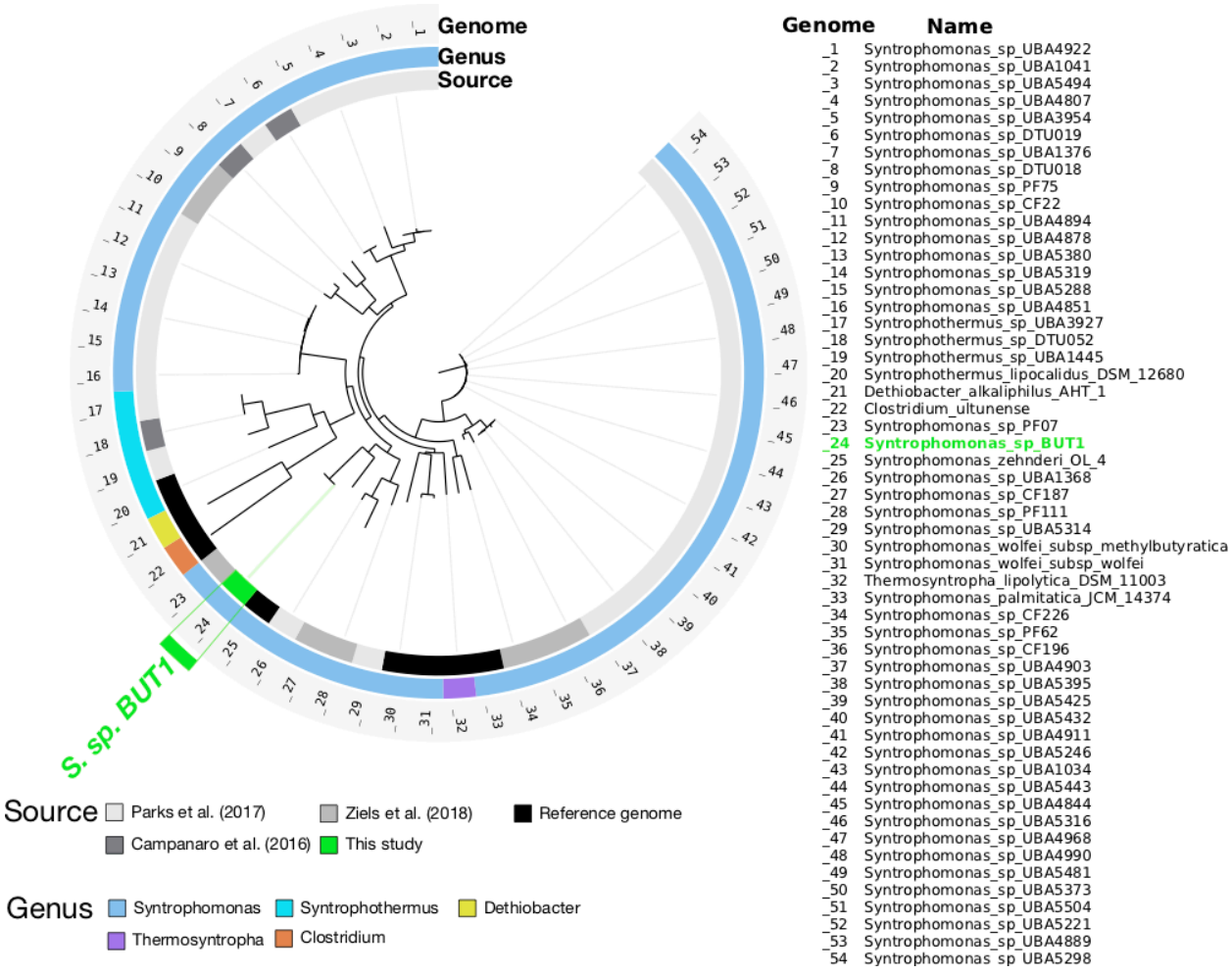

Figure 2: A phylogenomic tree showing the relationship of the ^{13}C-enriched *Syntrophomonas* BUT1 to other genomes available from the *Syntrophomonadaceae* family in the NCBI nr database (downloaded April, 2018). The tree is based on a concatenated alignment of 139 bacterial single copy marker genes (75) obtained using Anvi'o (72). Open reading frames were predicted with Prodigal v.2.6.3 (69), and queried against database of bacterial and archaeal single copy marker genes using HMMER v.2.3.2 (76). The tree was calculated using FastTree (77). The *Clostridium ultunense* genome was used as the outgroup.

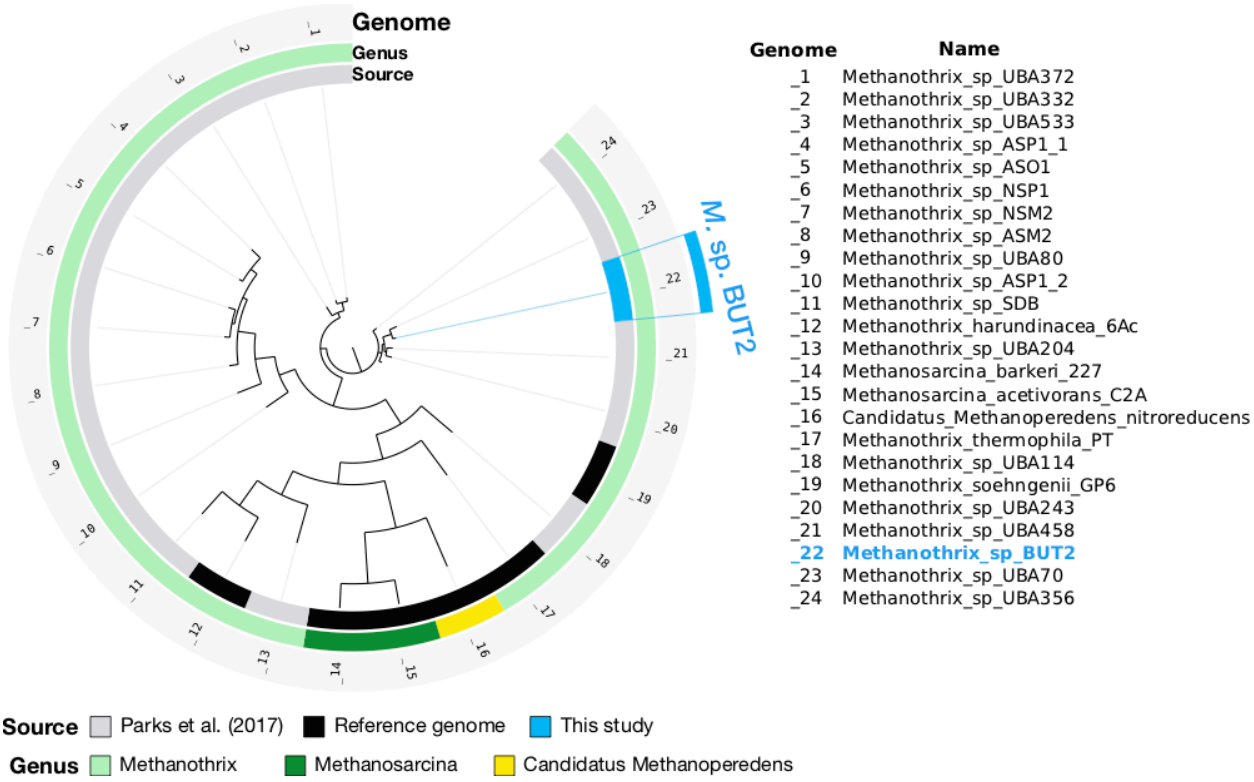

821

822 **Figure 3:** A phylogenomic tree showing the relationship of the ^{13}C-enriched *Methanothrix* BUT2
823 to other genomes within the order *Methanosarcinales* in the NCBI nr database (downloaded April,
824 2018). The tree is based on a concatenated alignment of 162 archaeal single copy marker genes
825 (78) obtained using Anvi'o (72). Open reading frames were predicted with Prodigal v.2.6.3 (69),
826 and queried against database of bacterial and archaeal single copy marker genes using HMMER
827 v.2.3.2 (76). The tree was calculated using FastTree (77). The *Candidatus* Methanoperedens
828 nitroreducens genome was used as the outgroup.
829

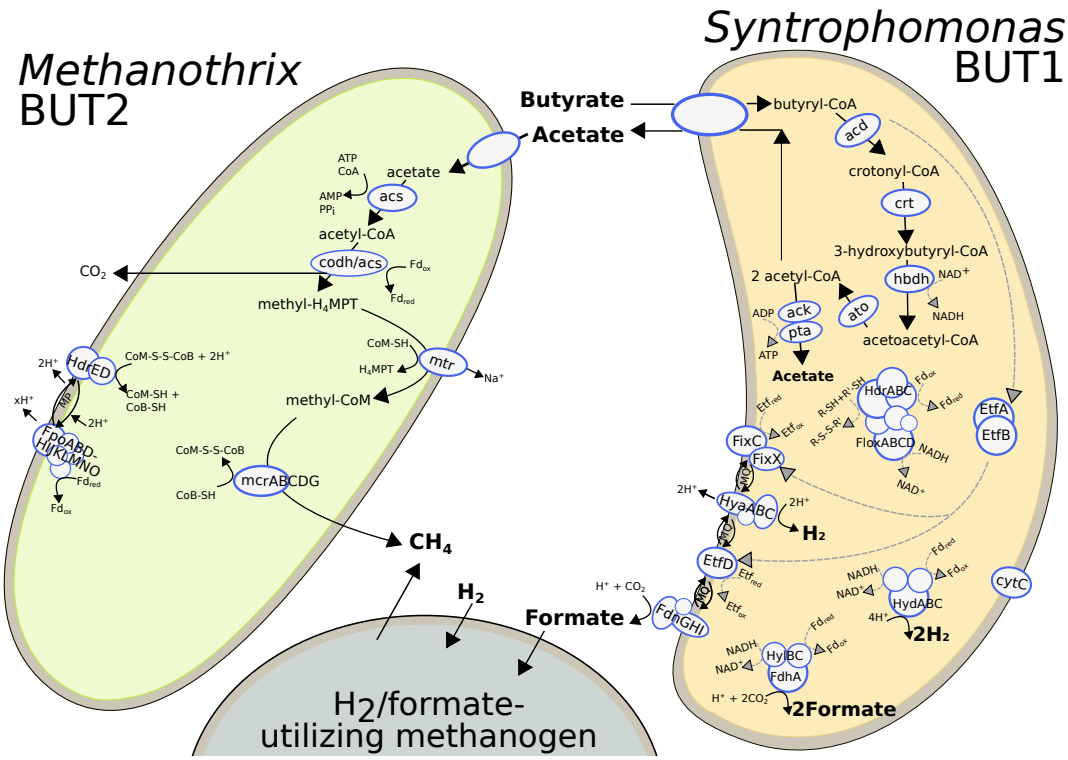

Figure 4: Cell diagram showing detected metabolic pathways for anaerobic butyrate degradation in syntrophic cooperation between *Syntrophomonas* BUT1 and *Methanothrix* BUT2. Abbreviations of enzymes are defined in Supplemental Files 2 and 3. The H_2/formate utilizing methanogenic partner is shown for conceptual purposes, but was not identified with ^{13}C-DNA SIP this study due to their autotrophic growth in the microcosms.